Research and Development of an Integrated Electro-Optical and Radio Frequency Aperture[1]

G. Logan DesAutels, Byron M. Welsh
And Peter Beyerle
Mission Research Corporation
3975 Research Blvd.
Dayton, OH 45430
(937) 429-9261
ldesautels@mrcday.com
bwelsh@mrcday.com
pbeyerle@mrcday.com

Abstract – Due to the fact that real estate on specific platforms (i.e. physical space on an aircraft) is already very crowded, it is difficult to house the many optical sensors, antennas or other sensor components onto such tight-spaced platforms. Therefore, in this paper, an Electro-Optical (EO) system has been integrated with a Radio Frequency (RF) sensor to enable both EO and RF sensors to utilize the same real estate. Both sensors employ the same RF horn as a common aperture. The EO system consists of a liquid crystal spatial light modulator (LCSLM), a power turning beam splitter and a laser source. The LCSLM is used to induce a modulated wavefront onto the laser to steer, focus, filter aberrations (atmospheric or lens aberrations) and form images, which ultimately propagates through the RF/EO aperture (RF antenna horn). The EO and RF systems were each characterized before being introduced to each other, and after, as one system to ensure the two sensors could co-exist. EO analyses were performed for optimal optical performance. Matlab algorithms were used to characterize the performance of the EO system before and after the RF aperture was introduced. Likewise, for the RF aperture, S11/VSWR and S21/gain tests were performed with and without the EO aperture/mirror.

TABLE OF CONTENTS

1. INTRODUCTION

For all advanced aircraft, available real estate for avionics systems is very crowded. It is very difficult to fit optical windows, antennas or other sensor components into increasingly tight-spaced areas. This has been a major concern for RF systems, which constitutes the bulk of the sensors and systems requiring real estate. This fact has been the driving force for the design of multifunction RF/EO apertures.

Combining two sensors into a common aperture has been achieved using a RF horn antenna and an EO beam steering/formation system. The EO system is comprised of a spatial light modulator, a laser and a power beam splitter that directs the laser to the SLM. Both the RF antenna horn and EO system have been examined to observe their performance alone and with modifications.

1.1. The Experimental Setup

The RF/EO aperture developed in this study is shown in Figure 1.

[1] 0-7803-7651-X/03/$17.00 © 2003 IEEE

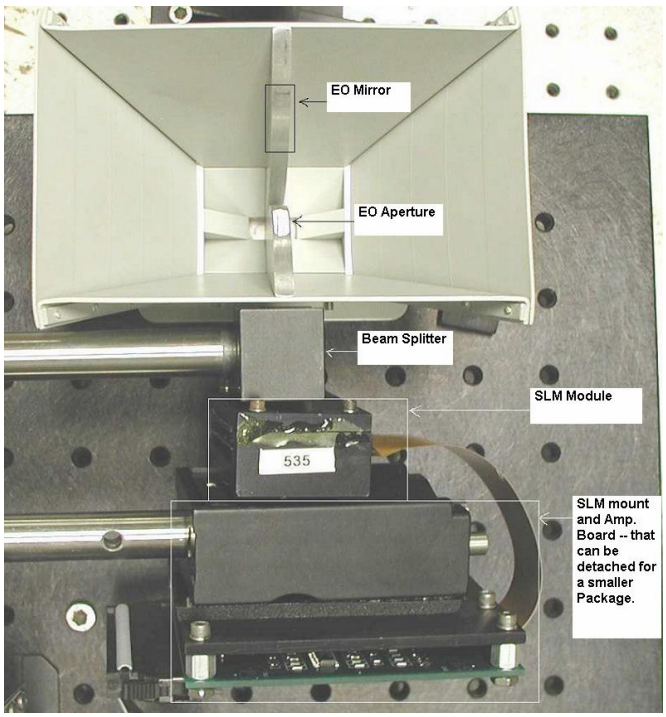

Figure 1. RF/EO integrated aperture illustration. The RF horn has an EO aperture through one horn vein and an EO mirror on the other vein. The SLM and beam splitter are coupled to the horn.. The laser is not shown, it is to the right of the picture.

This setup, in Figure 1, may be more easily illustrated graphically. Figure 2 presents another view of the setup. Figure 2, is a drawing that depicts multiple rays (solid and dotted) exiting the RF aperture. The solid rays represent the rays that reflect off of a flat EO mirror, and the dotted rays represent the rays reflecting off of a convex EO mirror, which provides a greater EO FOV.

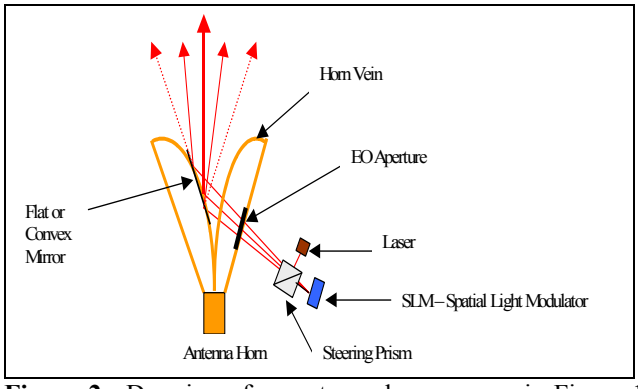

Figure 2. Drawing of an antenna horn, as see in Figure 1, with the EO beam-steering system. A laser illuminates the SLM through a power splitter.

The EO/RF integrated system includes a laser that is modulated by the SLM (modulation that steers or shapes the beam). The modulated light then encounters a flat or convex mirror that is bore-sighted to the RF horn aperture.

1.2. Ray-trace Analysis

A ray-trace analysis was performed, which provided information about the RF/EO aperture optical train. This involved modeling the RF aperture (horn antenna) veins and tracing rays through the RF aperture to provide the design and location of the EO aperture and mirror (flat and convex). The EO aperture is located on one of the RF veins, while the EO mirrors are on the other RF vein (separate mirrors on separate veins). The ray-trace analysis, therefore, determines the location of the EO beam steering system relative to the RF aperture.

1.3. FOV Analysis

A field of view (FOV) analysis was performed. This analysis was done to confirm that the convex mirror, designed in the ray-trace analysis, improves the FOV of the steered beam.

1.4. RF Analyses

RF tests were done to characterize the RF aperture before and after each modification. The modifications entailed an EO aperture and an EO mirror. These tests consist of a S11/VSWR measurement and a S21/Gain measurement, which will be explained in more detail later.

1.5. EO Analyses

The EO tests involved modulating the laser beam's wavefront with the SLM, then propagating that wavefront through the RF/EO aperture. The modulated wavefront forms an intensity pattern (image) on a CCD camera. The CCD camera is located after the RF/EO aperture. The images, after being recorded by the CCD camera, are analyzed in MATLAB. The analysis is done by correlating a theoretical target image to the image collected with and without the presence of the RF aperture.

1.6. Results

The results have shown that the modifications made to the RF aperture, horn antenna, did not alter the RF performance. The horn was first tested/characterized (S11/S21 measurements) as soon as it was received from the manufacturer, before any modifications. It was then modified with an EO aperture through the side of the horn and one of the veins. The results did not vary from the baseline (pre-modified) results. Next, the EO mirror was fabricated onto the other vein and the S11 and S21 measurements were repeated. The EO mirror also did not affect the RF aperture's performance. The results will be shown in greater detail later in this paper.

The results also show that the introduction of the RF aperture into the optical path does not significantly alter the EO performance. The EO system produced images of basic

geometrical shapes that were analyzed carefully to observe any variations in those images before and after introducing the RF/EO integrated aperture. The analysis consisted of correlating an ideal target image (described later) with the measured image and plotted verses target location. The plots given demonstrate how the correlation varies with different beam steering positions. At each location a correlation between that measured image and the ideal/predicted image was done. The correlation plots were then compared with and without the presence of the RF aperture. The correlation ranges from 0 to 1, where 1 is a perfect correlation. The comparison between these plots does not show any significant changes in performance.

2. Spatial Light Modulator (SLM)

The SLM was selected as the EO sensor because it primarily provides a means to non-mechanically steer a laser beam through the RF aperture. As mentioned, the SLM alters the phase of the laser beam to steer the beam, focus the beam, correct for atmospheric/optical aberrations or form images onto the beam. The SLM offers another interesting benefit to this study. It is a unique device that consists of electronic circuitry and an array of Electro-Optic liquid crystal (LC) material. Both the electronics and liquid crystals may be adversely affected by RF energy, which also needs to be determined. Therefore, the SLM is a suitable candidate for this study since it can steer an optical beam through the RF aperture and because of its unique physical makeup of electronic circuitry and optical LC material that can be studied in the presence of a RF field.

The SLM used is a liquid crystal spatial light modulator from Boulder Nonlinear Systems Incorporated[1]. This device is used to control the wavefront of the optical beam. The SLM transforms the planar wavefront into the desired phase front using a beam shaping phase retrieval-based wavefront control algorithm[2]. It is a reflective pneumatic liquid crystal device, operating in a phase only mode; in other words, it only alters the phase of the input wavefront and not the amplitude. This SLM requires linearly polarized illumination from the source. It is a reflection SLM, which means that a light source is incident onto the SLM at some angle and is reflected off with the phase, of the incident source, altered by the liquid crystals. Each liquid crystal is 6.14 microns square with 0.86-micron spacing in-between each pixel. The SLM has a pixel pitch of 7 microns, a fill factor of 77%, and 53% efficiency. The SLM has a frame rate is 25-50 Hz and an optical response times of 0.5-2.0 ms rise and 1.0-40 ms fall. The frame rate and optical response are both dependent on the wavelength, temperature and phase stroke. The SLM has a custom v-coated anti-reflection cover glass (standard cover glass uses a broadband AR coating yielding < 1% average reflectivity for 450-850-nm or 850-1600-nm). This device is designed to give maximum modulation at 632.8-nm. Other wavelengths can be used, but modulations of the wavefront will degrade. The device has a maximum steering angle of 0.647 degrees from center. A picture of the SLM is given in Figure 3.

The SLM has the ability of focusing/diverging a beam to any focal length desired. This ability enables the user to instantaneously change the focus, image or steering angle to meet the mission needs. Writing a lens phase function will focus or diverge the beam. Writing a blazing phase function, or grating, to the SLM enables the steering to occur. The user may write any addition phase function to the SLM, such as, an atmospheric filter to correct for aberrations caused by the atmosphere. All phase functions are simply added together.

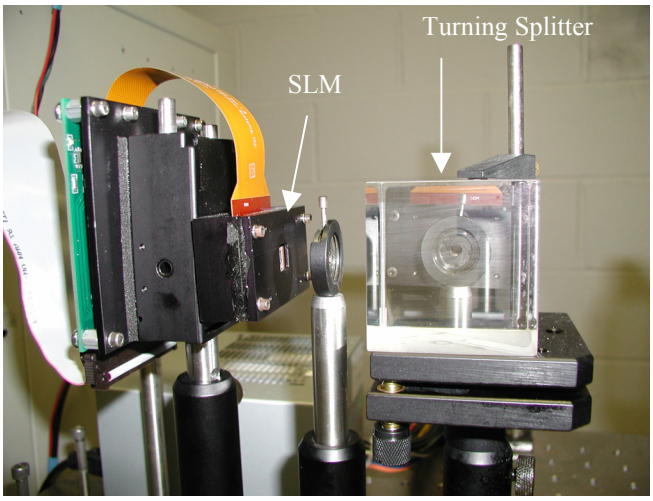

Figure 3. This figure shows a picture of the SLM in a former setup. A turning power splitter is used to direct the planar laser wavefront to the reflective SLM.

3. EO Studies

This section includes the ray-trace analysis results, which give the design, location and size of the EO aperture and mirrors (flat and convex). Also in this section will be a field of view (FOV) analysis done on the two EO mirrors designed in the ray-trace analysis. The convex mirror was design to provide an enhanced FOV for the EO beam steering system, which is one of the benefits of using the RF antenna horn as the RF aperture in this study.

3.1. Ray-trace Analysis

In this study, an algorithm was written using MATLAB to propagate the beam from the SLM through the RF/EO integrated aperture. The ray-trace analysis determined the best location and size of the EO aperture, which then defined the slope, size and location of the EO mirror. The veins were modeled in Matlab to perform this ray-tracing analysis, see Figure 4 or Figure 5. The results of the ray-trace analysis illustrate how the EO aperture is precisely drilled through one side of the horn and through one vein. The veins are 3.83” in length and the aperture is centered at 3.0”, which is near the top of the horn where only the low-end frequency range will be affected. The veins are 0.26”

thick and the aperture is 0.16” wide, therefore, ±0.05” is left on either side of the vein – this allows plenty of material for the RF wave to propagate along that vein. The opposite vein has a 0.5” long flat (or convex) mirror polished onto the surface in line with the EO aperture. Colorado Precision Products, Inc. (CPPI)[4] fabricated the 0.5” mirror.

Below are some MATLAB output plots of the RF horn veins with the flat and convex mirror surfaces. The output plots show the optical path from the SLM through the RF/EO integrated aperture.

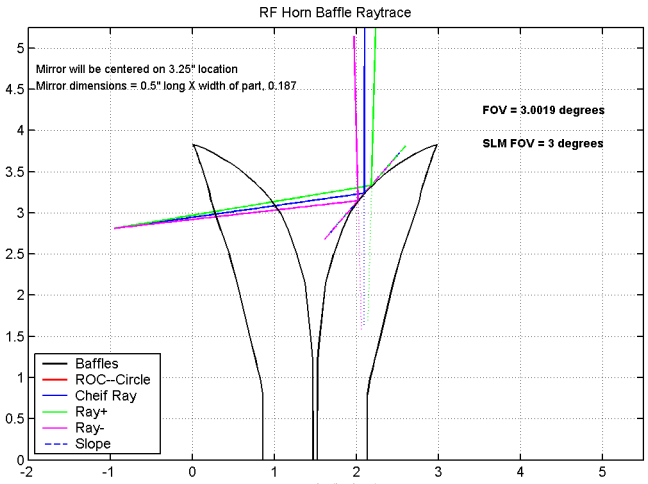

Figure 4. Ray-trace using MATLAB with the height (inches) verses the width of the parts (inches). A 0.5” flat mirror was polished on the right vein, while the EO aperture was drilled through the left vein as shown. The FOV equals the SLM FOV for this configuration.

Figure 4 is the ray-trace for a flat EO mirror. The FOV of the rays reflecting off of this mirror is the same as the SLM FOV. The SLM has a given steering angle, or FOV, which is inherent in the design of the device. The FOV of the SLM is dependent on device design, liquid crystals visco-mechanical properties, and grating efficiency[3]. However, Figure 5 demonstrates how a convex mirror can improve the FOV by an order of 3 or even greater if desired.

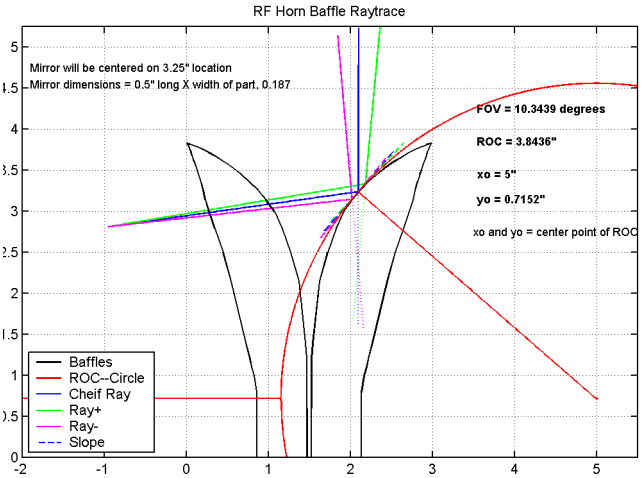

Figure 5. Ray-trace using MATLAB with the height (inches) verses the width of the parts (inches). A 0.5” convex mirror was polished on the right vein. The FOV is 10.35 degrees for this configuration.

Figure 5 illustrates an increased FOV with the use of a convex mirror instead of a flat on the right vein. The radius of curvature (ROC) of the convex mirror, in Figure 5, is described as the red circle encompassing the right vein. It can be a smaller circle, or ROC, which means a larger FOV. A ROC of 3.84” was chosen so that the diamond tool, in the diamond turning process, would miss the part (right vein). If the ROC were smaller, the red circle would encounter the top and bottom of the right vein.

3.2. FOV Analysis

In this analysis, flat and convex EO mirrors were compared. The mirrors were fabricated on two separate horn veins and each tested in the same horn and identical setups. The setup for this experiment is shown in Figure 6.

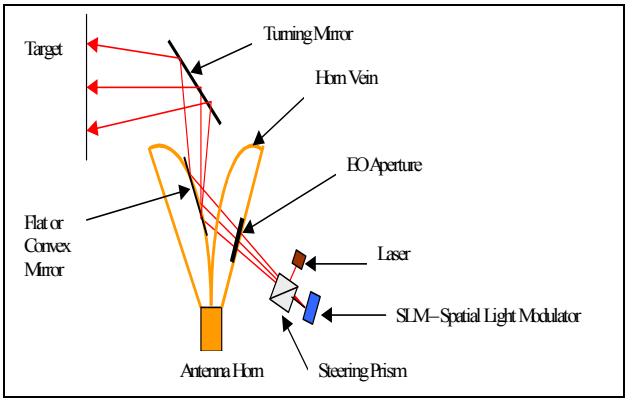

Figure 6. Setup for FOV experiment. Two horn veins were fabricated, one with a flat mirror and the other with a convex mirror. The setup remained constant while the mirrors were interchanged.

The results are shown in Table 1 below.

Table 1. FOV experimental results.

EO Mirror	Distance From SLM To Target	Distance Between Steered Target Positions	Steered Angle	FOV
Flat	297.18 mm	8.89 mm	1.71°	3.42°
Convex	297.18 mm	26.67 mm	5.13°	10.26°

Table 1 presents the FOV data for the flat and convex mirrors. The convex mirror FOV is as predicted, ~10.3°, but the flat mirror (or SLM) FOV is slightly off. This is probably due to underestimating the FOV of the SLM in the ray-trace analysis. The maximum steering angle of the SLM, given by the manufacturer (BNS), may be slightly different for each SLM produced. Aside from this, the FOV has successfully been improved using a convex mirror fabricated onto the horn vein. The SLM can remove the spreading of the beam by writing an additional phase map to the SLM knowing the ROC of the convex mirror. This will allow for an increased FOV while maintaining the desired beam shape.

4. EO RESULTS

This section will provide the data results for the EO sensor with and without the presence of the RF aperture. However, first, Figure 7 demonstrates to the reader the optical path of the RF/EO integrated aperture. In Figure 7, the beam is propagating to the beam splitter, to the SLM, back through the splitter and through the RF/EO integrated aperture.

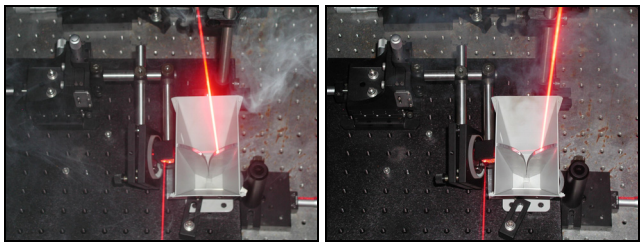

Figure 7. This figure demonstrates how the modulated beam would steer through the RF/EO integrated aperture. A flat mirror is being used as a placeholder for the SLM only for demonstration proposes.

The EO results are presented as images of some basic geometrical shapes that were used to analyze the performance of the EO sensor/system. These images are initially phase maps, generated with MRC's phase retrieval algorithm, which the SLM uses to generate an image from the laser planar wavefront at the image plane. The following images used in this analysis are given below:

1. Alien = "fun" visual image.
2. Batman = "fun" visual image.
3. Plus sign = image to be analyzed.
4. Square = image to be analyzed.
5. Triangle = image to be analyzed.

The "fun" images are presented to show the reader, one, how well the SLM device forms images and two, to give a good visual comparison of the "fun" images with and without the RF aperture. The remaining geometrical images are used to perform the correlation analysis, but also give a visual comparison.

Figure 8 gives a comparison of the "fun" images with and without the RF aperture.

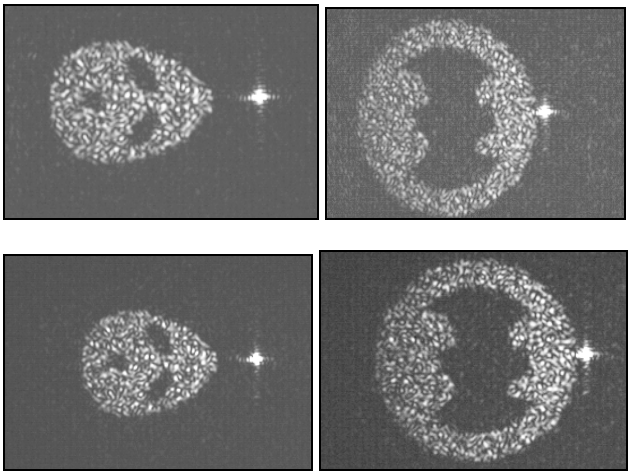

Figure 8. Results for "fun" images with and without the RF aperture. Top left) alien without the RF aperture, top right) batman symbol without the RF aperture, bottom left) alien ***with*** the RF aperture, bottom right) batman symbol ***with*** the RF aperture.

Figure 8 illustrates that the RF aperture indeed does not appear to have a visual affect on the EO system. The "dot" in the center of each image (Figure 8, Figure 9 and Figure 11) is an artifact of the SLM resolution. It is called "dead-space" and is the result of a Fourier Transform of the grid pattern of empty space between active pixels. This artifact is not being analyzed.

Figure 9 and Figure 11 show the geometrical images that are analyzed visually as well as qualitatively with correlation plots.

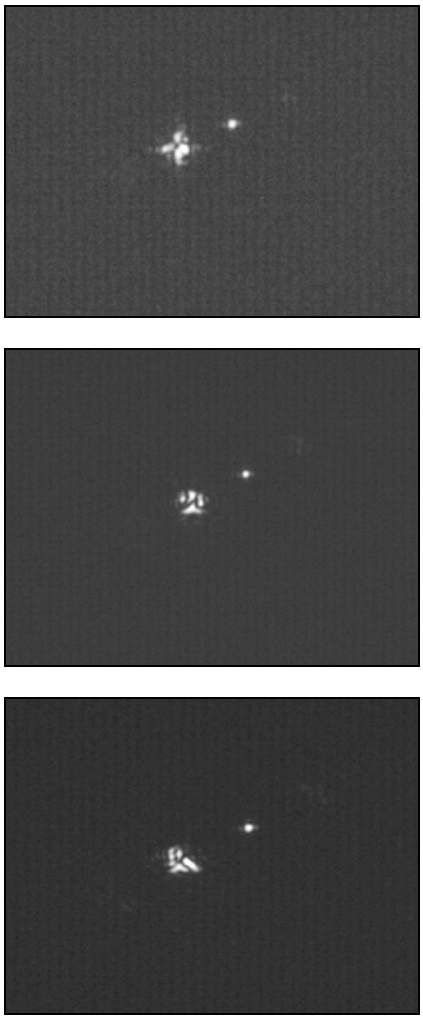

Figure 9. Geometric images ***without*** the RF aperture. Top) a plus sign steered at off center, middle) a square steered off center, bottom) a triangle steered off center.

Figure 9 represents only one of five data points, for each geometrical image, that is compared with an ideal target image. The ideal target images are given in Figure 10.

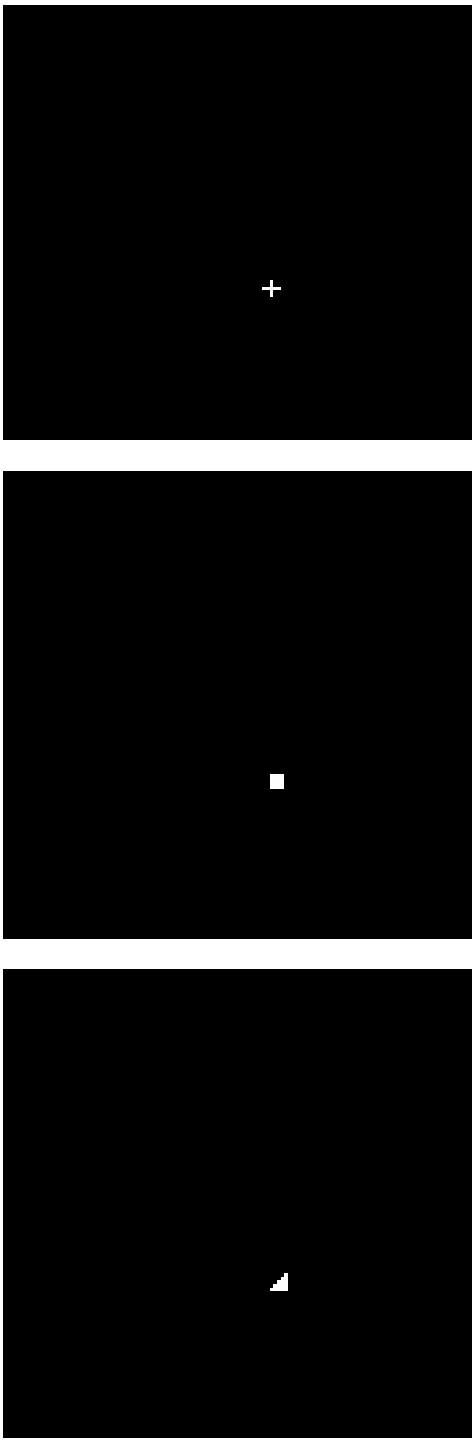

Figure 10. Ideal target images of the geometric shapes to be compared with the data in Figure 9 and Figure 11.

Figure 10 shows the ideal or target images that both of the data sets (data in Figure 9 and Figure 11) are compared with. Correlation plots were produced of the target images with the data *without* the RF aperture as well as the data *with* the RF aperture.

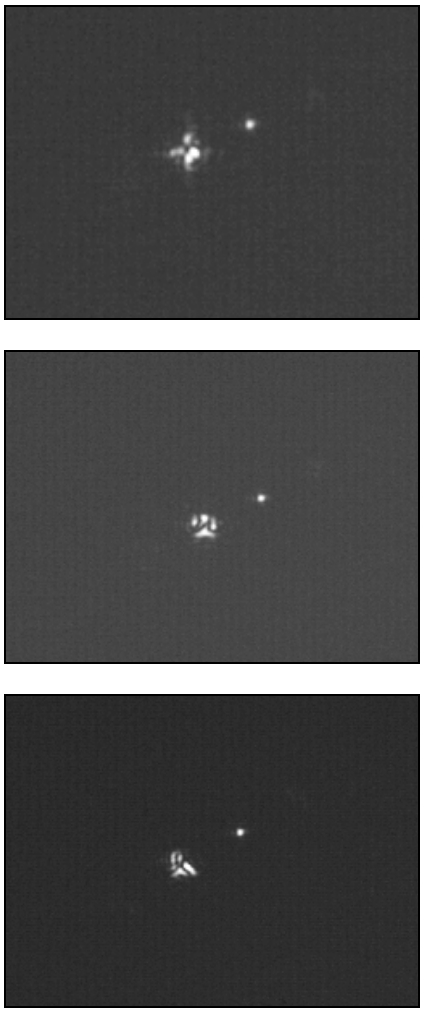

Figure 11. This figure displays the data of the geometrical shapes ***with*** the RF aperture.

Figure 12 shows the correlation plots between the target images and the data, with and without the RF aperture.

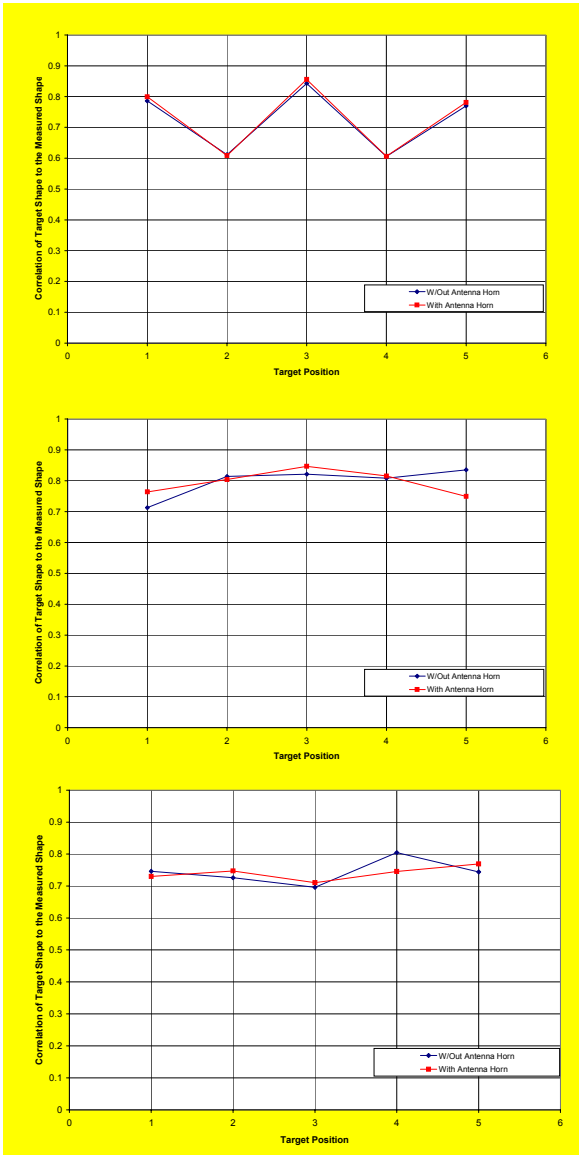

Figure 12. This figure shows the correlation of an ideal target with each of the geometrical images collected *with* and *without* the RF aperture. It is a plot of the Correlation of Target Shape to the Measured Shape (ranging from 0 to 1) verses the Target Position (geometrical targets measured at five different locations). The red trace is the measured data with the RF antenna horn, and the blue trace is the measured data without the RF antenna horn. Top) Plus sign images at five different locations, Middle) square images at five different locations, Bottom) triangle images at five different locations.

The data was collected in Figure 12 by recording the geometrical targets at five different target positions. The position of each target was changed ~10 pixels diagonally from the center of the bitmap image. A phase map of each bitmap image was created from the MRC phase retrieval algorithm, and imported into the SLM's driver. The SLM then uses this phase map to alter the laser beam's planar wavefront. The altered wavefront then propagates through

the RF aperture, or antenna horn, and to the CCD camera were the image is recorded.

Figure 12 gives similar results as the visual data outputs. That is, no significant EO alterations with or without the RF aperture. The variations that do occur are due to the slight re-alignment of the optical train after the antenna horn was added.

5. RF RESULTS

In this section, the RF baseline and modified results are presented. The RF baseline is the data without modifications to the horn (e.g. EO aperture/mirror). The RF horn, directly from the manufacturer without any alterations, was tested with S11 and S21 type measurements. The EO aperture was then introduced and S11/S21 tests were again performed. Finally, the EO mirror was added and the S11/S21 measurements were taken again. Data was acquired from 2 to 18 GHz, but only the 2 GHz, 10 GHz and 18 GHz vertical polarization data will be presented. The measurements performed are the S11 and S21 type measurements. These types of measurements are explained in detail below:

- S21/Gain:
  - This is a measure of the antenna's ability to receive a signal. This measurement can be done using a NA, but it was done in the MRC compact RF range to isolate the antenna and source from the outside world/interference. Inside the range there is a calibrated monopole RF source (a collimated source) emitting a signal at some distance from the antenna horn. The horn was rotated ±90 degrees in x and y-axes. The frequency range was 2-18 GHz at 0.25 GHz increments. The signal/data that is received by the horn antenna is used to generate plots of gain (dB) verses angle (degrees) – these plots are referred to as antenna patterns.

  - This measurement is used to characterize the antenna horn's receiving capabilities before and after the EO aperture/mirror.

- S11/VSWR/Log Magnitude:
  - This is a measure of the return loss (or impedance mismatch) of the RF signal using a network analyzer (NA). The NA sends a small RF signal (over a range of frequencies) across a 50-ohm line to the antenna in question. If that antenna does not have impedance of exactly 50-ohms, part of the transmitted wave will be reflected back to the NA where it is measured. This reflected energy is then plotted as loss (-dB) verses frequency for an S11 measurement, or plotted as normalized loss (where a perfect impedance match equals 1) verses frequency for a VSWR measurement.

  - This measurement was performed, before alterations, to characterize how well the RF antenna horn's impedance is matched with the NA 50-ohms RF line. After the EO aperture was added the S11 measurement was performed and compared to the baseline. This measurement was repeated when the EO mirror was added.

A portion of the RF results is presented in Figure 13 and Figure 14 below.

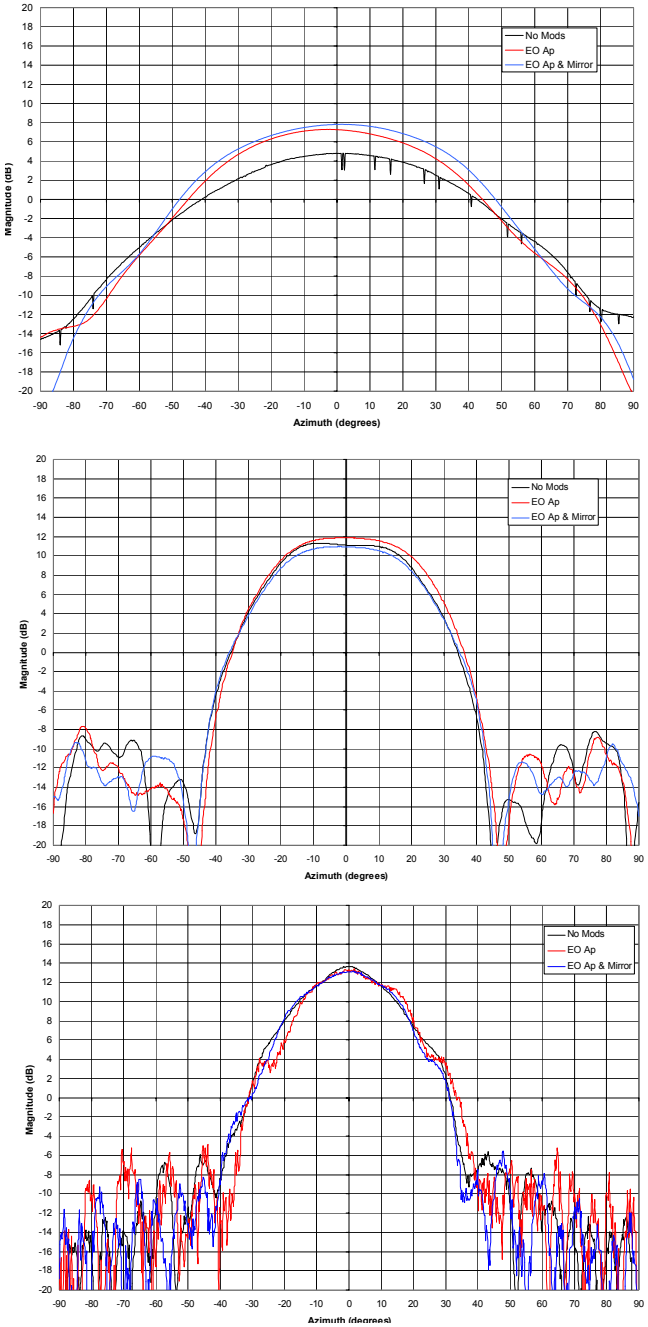

Figure 13. The Phase I horn S22/Gain pattern for the Vertical Polarization. The gain (dB) is plotted versus aspect angle for various frequencies (2-18 GHz). The various colored curves in each plot were measured before and after the horn was modified. The black trace is the horn without modifications. The red trace is the horn with the EO

aperture, and the blue trace is the horn with the EO mirror added. Top) 2 GHz data, middle) 10 GHz data, bottom) 18 GHz data.

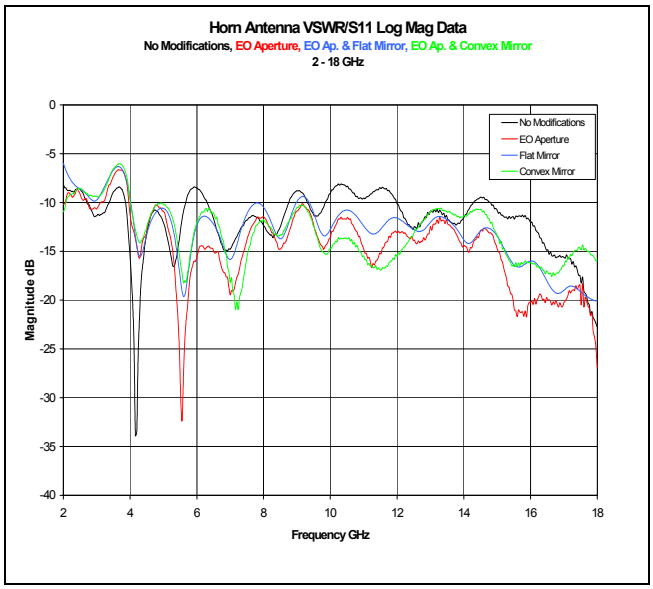

Figure 14. The RF horn return loss as a function of frequency. Three traces: black) horn without any modifications, red) one modification – the EO aperture, blue) EO mirror added. The axes are Magnitude (dB) verses Frequency (GHz).

The charts in Figure 13 and Figure 14 do not show any "real" affects from the EO aperture and mirror. The changes in the traces are primarily due from re-assembly of the antenna horn after being disassembled to replace the factory veins with MRC manufactured veins (EO aperture vein and EO mirror vein). Figure 14 actually represents improved performance, from the unmodified horn, when the EO aperture was added. The performance degraded slightly when the EO mirror was added, but it is still better than the original. Overall, the EO aperture and mirror had very insignificant effects on the RF horn.

6. CONCLUSION

Space onboard advanced aircraft platforms is very limited. There are many sensors that are necessary or wanted for various missions, which are unable to fit onto the aircraft together. In this Phase I effort, an EO system was integrated with a RF aperture to conserve aircraft real estate. The EO/RF sensors employed the same aperture and the two sensors performed successfully. The experimental data presented indicates that: 1) an EO aperture does not affect the performance of the RF aperture, 2) an EO mirror does not affect the performance of the RF aperture and 3) an EO sensor has not shown any adverse affects from being coupled to the RF aperture.

REFERENCES

[1] Boulder Nonlinear Systems, Inc., Lafayette, CO. Developed and manufactured the 512x512 Liquid Crystal Spatial Light Modulator. Phone: (303) 604-4466.

[2] Brad R. Stone, Byron M. Welsh, Mike C. Roggeman. "Far Field Beam Shaping and Steering Using Phase Retrieval-based Wavefront Control". *Proceedings* SPIE, Vol. 4124, July 2000.

[3] Paul F. McManamon, Terry A. Dorschner, David L. Corkum, Larry J. Friedman, Douglas S. Hobbs, Michael Holz, Sergey Liberman, Huy Q. Nguyen, Daniel P. Resler, Richard C. Sharp, Edward A. Watson, "Optical Phased Array Technology". Proceedings of The IEEE Vol. 84, No. 2, February 1996, Pages 268-298.

[4] Colorado Precision Inc., Boulder, CO. Flat and convex mirror fabrications. Phone: (303) 444-9711.